



HAL
open science

Computer simulation of performance of electrical discharge machining operations

José Antonio Sánchez, Borja Izquierdo, Naiara Ortega, Iñigo Pombo, Plaza Soraya, Itziar Cabanes

► **To cite this version:**

José Antonio Sánchez, Borja Izquierdo, Naiara Ortega, Iñigo Pombo, Plaza Soraya, et al.. Computer simulation of performance of electrical discharge machining operations. International Journal of Computer Integrated Manufacturing, 2009, 22 (08), pp.799-811. 10.1080/09511920902741125 . hal-00513414

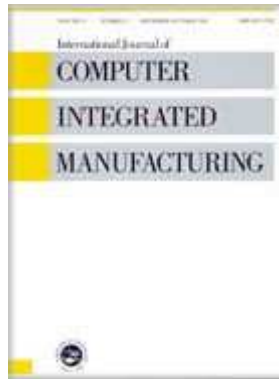
HAL Id: hal-00513414

<https://hal.science/hal-00513414>

Submitted on 1 Sep 2010

HAL is a multi-disciplinary open access archive for the deposit and dissemination of scientific research documents, whether they are published or not. The documents may come from teaching and research institutions in France or abroad, or from public or private research centers.

L'archive ouverte pluridisciplinaire **HAL**, est destinée au dépôt et à la diffusion de documents scientifiques de niveau recherche, publiés ou non, émanant des établissements d'enseignement et de recherche français ou étrangers, des laboratoires publics ou privés.



Computer simulation of performance of electrical discharge machining operations

Journal:	<i>International Journal of Computer Integrated Manufacturing</i>
Manuscript ID:	TCIM-2008-IJCIM-0063.R1
Manuscript Type:	Original Manuscript
Date Submitted by the Author:	17-Nov-2008
Complete List of Authors:	Sánchez, José Antonio; Faculty of Engineering of Bilbao, Mechanical Engineering Izquierdo, Borja; Faculty of Engineering of Bilbao, Mechanical Engineering Ortega, Naiara; Faculty of Engineering of Bilbao, Mechanical Engineering Pombo, Iñigo; Faculty of Engineering of Bilbao, Mechanical Engineering Soraya, Plaza; Faculty of Engineering of Bilbao, Mechanical Engineering Cabanes, Itziar; Faculty of Engineering of Bilbao, Mechanical Engineering
Keywords:	ELECTRO-DISCHARGE MACHINING, SURFACE MODELLING
Keywords (user):	thermal modelling, finite differences



Responses to reviewers and editor suggestions

- Reviewer 1:

Authors should compare their approach with related approaches reported in the literature. They should provide sufficient details on their model, such as the boundary conditions and how they are derived from the operating or physical parameters of EDM process. More specific comments pertaining to the aforementioned are given below:

1) The author should give a brief explanation of equation (1), or at least give nomenclature of the terms used in the equations.

- A brief explanation of equation (1) has been included, together with nomenclature of the terms:

‘Although as said before a large number of phenomena occur during the removal process, it is commonly accepted that the most important one is the thermal effect (Van Dijck 1974, Jilani and Pandey 1982, Erden 1983, Singh and Ghosh 1999). Therefore, basic modelling of the EDM process involves placing and solving the heat transmission problem (see Equation 1) assuming a heat input given by each one of the sparks that occur during machining. This equation represents a three dimensional time dependent heat transmission problem involving a heat input. In the mentioned equation k and α are the thermal conductivity of the material being heated and diffusivity respectively and \dot{q}_G represents the value of the heat input. For a given boundary conditions, the solution yields a temperature field from which the amount of part material that melt and vaporises can be predicted.’

$$\frac{\partial^2 T}{\partial x^2} + \frac{\partial^2 T}{\partial y^2} + \frac{\partial^2 T}{\partial z^2} + \frac{\dot{q}_G}{k} = \frac{1}{\alpha} \cdot \frac{\partial T}{\partial t} \quad (1)$$

2) “Figure Figure” repetition occurs in several places in the text.

- This has been corrected.

3) Page 9, line 21: *‘EDM experiments have been carried out under similar flushing conditions to those imposed on the above numerical simulation’*. It is not clear as to how the flushing conditions are employed in the simulation. Is this for a single discharge (e.g. how is the boundary condition at the interface with the dielectric fluid influenced by the flushing condition) or based on the distribution of dielectric over the surface of the tool and workpiece (as mentioned in the CFD simulation)?

- The aim of CFD simulation was to show that debris concentration has influence on the discharge process during EDM, as shown in our work. However, it is very difficult to implement this feature in a simulation software, so the validation proposed has been done under the hypothesis that optimum flushing conditions are used, which ensures

that debris is evacuated from the gap between electrode and workpiece. Special care has been taken during experimental tests to guarantee cleanliness in the dielectric medium. This has been explained in the revised text:

'EDM experiments have been carried out under similar flushing conditions to those imposed on the above numerical simulation. The EDM'ed surfaces have been measured using a contact profilometer (see section 4 for more details). The results, shown in Figure 6, reveal that more workpiece material is removed at the centre of the workpiece, where dielectric velocity is higher and therefore debris is more easily removed by the dielectric flushing. It can be concluded that important information can be extracted from CFD to include the effect of debris concentration in the model. As it has been said, the aim of CFD simulations was to show that debris concentration influences discharge characteristics, so discharges which take place in clean dielectric lead to different material removal rates and surface finishes than those discharges affected by high concentrations of debris. However, representing the effect of debris on EDM in a modelling of the process is very difficult. For that reason the validation of the present model has been performed on the hypothesis that the dielectric medium is clean. Tests carried out for the validation have been done under optimum flushing conditions taking special care to guarantee that the dielectric is clean in all the working area, and in the modelling tool it has been assumed that debris concentration is the same in all the points of the simulated surface.'

4) Page 9, line 9: the authors mention 'The definition of discharge location has also been included in the model. A probability function has been obtained so that for points whose distance to the electrode is short (peaks on the eroded surface)'. How and what kind of probability function is used and what is reason for the choice?.

- The probability function is based on discharge tests performed using stepped workpieces with different step heights, an explanation has been added:

'The definition of discharge location has also been included in the model. A probability function has been obtained so that for points whose distance to the electrode is short (peaks on the eroded surface) discharge probability is higher than that for points further from the electrode (valleys of the EDM-ed surface) (Kojima et al. 1992, Kunieda and Kiyohara 1998). This probability function is used to determine the element of the discretized surface on which the next discharge will take place. The mentioned function has been obtained from experimental results obtained in discharge test carried out on stepped workpieces. The aim of these tests was to count the number of discharges occurred in the top surface and in the lower surface of the stepped piece for different step heights. It was observed that as the step height increases the probability of discharge occurrence on the top surface tends to be 100%, while for low step heights it tends to be equally distributed (50% of spark occurrence in both low and top surfaces). Empirical results obtained with these tests were included in the model, in such a way that points of the eroded surface located closer to the electrode (peaks of the surface) have greater probability for discharges to take place on them.'

5) Page 10, section 4, the authors should define and mention how they measured the different roughness parameters, especially S_{dq} (root mean square of the topographic

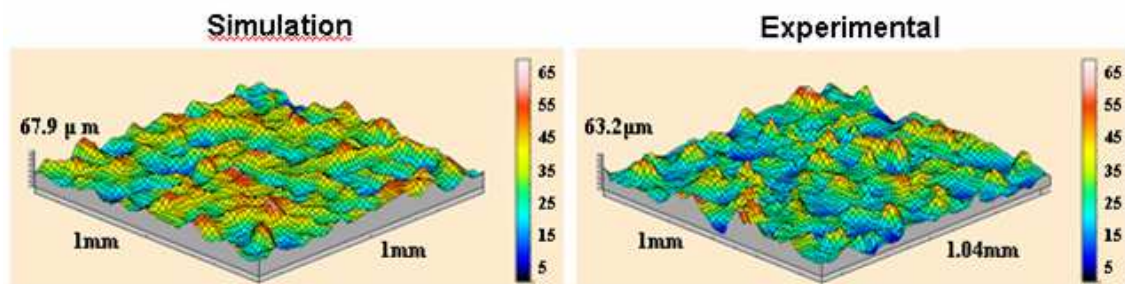
surface) and S_{dr} (developed interfacial area ratio) used in this study. They should also indicate whether they measure the parameters over the entire machined zone, or certain targeted area, and the instrument used to obtain the topography of the measured surface in Fig.9.

- Explanations about the instrument and the software used to obtain topographies have been added, as well as number and size of the analysed areas:

‘The experimental determination of these surface parameters of EDM-ed surfaces was performed with a contact profilometer (Taylor Hobson Talysurf Series 2) and with surface analysis software associated to the profilometer (TalyMap Expert 3.1.9). This software was also employed to analyse results of the simulations. Since the model generates surfaces of 1.2x1.2mm, experimental measurements have been performed in areas with the same size as simulated surfaces. Four measurements were carried out, each of them in a different location of the 30x30mm eroded surface and their mean value was used to compare experimental and simulated surfaces.’

6) In Figure 8 three different points with same S_a but different S_{dq} are shown, but no explanation given as to what it implies? Fig.9 is not clear (the labeling and scale are not legible).

- Figure 9 has been modified to make labelling and scale legible.



- Explanation about roughness parameters taken into account in this work is given below.

7) On page 10, the authors mention: “Figure 8 illustrates this fact, showing that surfaces with similar value of S_a may exhibit very different values of S_{dq} ”. However, the authors have not given any reason or explanation for this observation, e.g. in relation to the simulation results.

‘It must be taken into account that surface roughness parameters are defined statistically. The formulae for the calculus of these parameters are given below:

$$S_a = \frac{1}{MN} \sum_{k=0}^{M-1} \sum_{l=0}^{N-1} |Z(x_k, y_l) - \mu| \quad (10)$$

Where μ is the mean height of the profile:

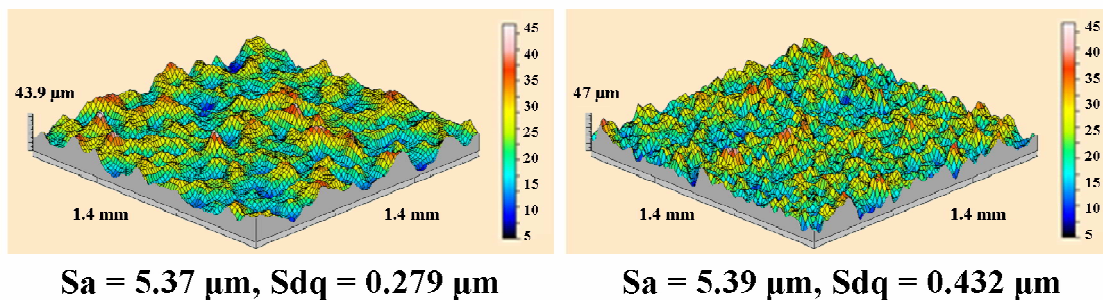
$$\mu = \frac{1}{MN} \sum_{k=0}^{M-1} \sum_{l=0}^{N-1} Z(x_k, y_l) \quad (11)$$

And the equation for S_{dq} is:

$$S_{dq} = \sqrt{\frac{1}{(M-1)(N-1)} \sum_{k=0}^{M-1} \sum_{l=0}^{N-1} \left(\frac{Z(x_k, y_l) - Z(x_{k-1}, y_l)}{\Delta x} \right)^2 + \left(\frac{Z(x_k, y_l) - Z(x_k, y_{l-1})}{\Delta y} \right)^2} \quad (12)$$

This means that two different surfaces that exhibit similar values of amplitude parameters (such as S_a , S_q and S_z) may produce different values of hybrid parameters (such as S_{dq} and S_{dr}). Of course, this is independent on the manufacturing process used to generate the surface. In other words, this is not an intrinsic property of EDM-ed surfaces.

As far as to the surfaces represented in Figure 9 refers, the one at the right has been generated using a low value of the plasma radius (input variable R_p) that produces small craters, whilst the one at the left has been generated using a higher value of R_p . The result is two different surfaces that exhibit similar values of S_a , but different values of S_{dq} .



8) The authors verified the model for a single set of experimental conditions. No comparison of theoretical and experimental MRR and surface roughness values for different machining conditions. The authors didn't mention whether their model is suitable for both rough and finishing regime. It is suggested that the authors can validate their model using more (3/5) different experimental conditions (both for roughing and finishing).

- At the present stage, the current work is focused on the adjustment of the model to different machining conditions. Of course, the model aims to be general, and suitable to both roughing and finishing conditions. Although still this work is in progress, we have carried out the adjustment for a finishing regime whose electrical parameters are given in Table 4. The following paragraphs have been included in the text:

'The present model aims to be general, and suitable for both roughing and finishing conditions. Although this work is still in progress additional simulations have been carried out for another regime, different to the one mentioned above. Electrical parameters for this regime are listed in Table 4 and the results of the comparison between predicted and experimental material removal rates and roughness parameters

are shown in Table 5. As for the other studied regime, the error in the predicted material removal rate is very low ($< 1\%$), while the error for the considered roughness parameters is lower than 10% except for S_{dr} . In this case the error is slightly higher, with a value of 13.78% , which still represents a good approximation.'

EDM conditions	
On-time (t_{on})	18.2 μ s
Off-time (t_{off})	6.5 μ s
Open-circuit voltage (U_0)	200V
Gap servo voltage (V_{gap})	25V
Discharge current (I)	6A
Electrode material	Copper
Dielectric fluid	EDM fluid GR2 (by Steelfluid)
Flushing	External

	Q_w	T_{eq} [$^{\circ}$ C]	R_p	S_a [μ m]	S_q [μ m]	S_z [μ m]	S_{dq} [μ m/ μ m]	S_{dr} [%]	E_s	MRR [mm^3/min]	$Error$ MRR [%]
SIMULATION	0.075	2000	502	3.073	3.84	24.21	0.362	6.44	0.0411	4.5	0.24
EXPERIMENTAL	-	-	-	3.33	4.215	26.35	0.344	5.66	-	4.52	-

9) In section 5, the authors discuss the 'Analysis of the influence of the input variables on the accuracy of the model' and also the contribution of different parameters on the performance. There is no comparison with what has been reported in the literature with regard to the influence of these parameters (e.g. 'In this case it is clear that the most influencing factor is R_p , while Q_w and T_{eq} have no influence on these surface parameters'). There is also no comparison or discussion with regard to other models mentioned in the literature.

The literature survey shows very limited information concerning the influence on surface roughness and material removal rate of parameters such as radius of the discharge channel, equivalent temperature or percentage of heat transferred to the workpiece. Only scattered data about the influence of discharge current and pulse duration can be found, and these data have been obtained from single discharge models. Therefore, no comparable models (this is, multidischarge models that account for the above mentioned parameters) can be found in literature.

Even though, the general trends observed both in experiments and in previous models are confirmed by the original model proposed in this paper: the higher the energy input, the higher the material removal rate obtained; if the radius of the plasma channel is very high a low efficiency of the process is achieved, since most of the heat is used to heat the workpiece (a large heat affected zone is produced, in comparison with small radii that concentrates the heat), but not to remove material. A similar effect is observed with the pulse duration (on-time). These observations can be found in the works by Jilani (1982), Pandey (1986), Ben Salah (2006), Natsu (2006), Kojima (2007) and Yeo (2007) that are already included in the references of the paper.

10) In section 5 the authors indicate that “In the validation of the model, data extracted from literature have been used.” However, in other sections (abstract, introduction, conclusion etc.) they indicate that, experiments using industrial EDM machine have been conducted to validate the model. The authors should be clear as to these apparently conflicting statements.

- Data extracted from literature have been used to establish the values for the input variables of the model for the selected erosion regime, and results obtained from the simulations have been compared with experimental measurements to perform a validation of the model. The text has been slightly modified in order to offer a better explanation of this feature of our work.

‘As commented in the review of the State-of-the-Art, the model is governed by the variables that define the partition of the discharge energy (Q_w), the geometry of the heat source (R_p), and the volume of part material actually removed per discharge by melting and vaporising (T_{eq}). In the validation of the model, data extracted from literature have been used to establish the values of the considered input variables before performing simulations. Results of simulations have been compared with experimental machining tests to validate the proposed model (as explained in section 4). However, these data correspond to a given EDM regime, and therefore will vary for other regimes. In order to evaluate the influence of these inputs on the accuracy of the model a systematic study was carried out. A two-level, four-factor full factorial experiment design was chosen. The factors are Q_w , T_{eq} , R_p and the exponent of the Gaussian heat flux distribution, and for each combination of input parameters three simulations were made, to consider the stochastic nature of their results. Table 4 shows the performed simulations and their results expressed using the mean value of the three simulations carried out for every parameter combination.’

11) In Page 11, section 5 the authors mention that “However, these data correspond to a given EDM regime, and therefore will vary for other regimes”. Clarify the term “regime”.

- When we refer to an EDM regime or erosion regime we are talking about a particular set of machining parameters governing the process, such as discharge duration, pause time, discharge voltage and discharge intensity. This has been clarified in the text:

‘From the above results interesting conclusions can be drawn. On the one hand, the input values of T_{eq} , Q_w and R_p are responsible for important differences in the accuracy of the model and therefore their values must be set for any different EDM regime, this is, for other machining parameters or materials. On the other, the exponent of the Gaussian distribution has a negligible influence on the accuracy of the model, and therefore its value can be set at -4.5 as recommended by other authors in the literature.’

- Referencing:

1) Not in numerical order, after reference 10, it's 20 on Pg. 4

- This has been corrected.

2) Proposed reference related to PhD dissertation by Van Dijck has been included.

- Typological and Grammatical correction:

1. Page 4, section 1, last sentence of the second last paragraph, 'full stop is missing to finish the sentence'.

2. Page 6, line 10, 'The thermal models commented before focus on the scientific description of the phenomena involved, **basin on** the analysis of a single spark'. The sentence is not clear, 'basin on' should be replaced by 'based on'.

3. Page 6, line 11. 'it must **bee** take into account' should be 'must be'.

4. 'The mathematical description of the model is included in Section 2 Discharge location has also been considered in this new model'. Use full stop after Section 2 to remove ambiguity.

5. Page 9, line 18, it was stated that 'The results of the simulation, shown in Figure Figure 5, reveal higher velocities at the centre of the workpiece'. No need to write the word 'Figure' twice. Correct the same mistake through out the document.

6. Page 12, line 9, full stop is missing to end the sentence.

- These corrections have been made.

- Reviewer 2:

1) This manuscript presents computer simulation model of the EDM process, which aims to predict material removal rate and the surface roughness.

2) Please check spelling and grammar

- Grammar and spelling have been corrected following the comments of both reviewers and editor.

3) Is Equation 2 missed?

- Equation 2 is included in page 5:

'As far as to the geometry of the heat source concerns, its size and shape have to be simulated. Early analytical models considered a point source, but all the recent

models assume that the heat source has a disk shape. Although some authors considered that the shape of the plasma channel remains constant during the discharge, Pandey (1986) obtained an equation to calculate the plasma channel, that grows showing a steep increase in the diameter in the first microseconds of the discharge and a posterior stabilization. It also showed its dependency on material's physical properties. Das (2003), Descoedres (2005), Natsu (2006) and Kojima (2007) made optical observations using high speed framing cameras that corroborate the initial fast growth and later stabilization. This experimental observation is commonly expressed mathematically using Equation 2:

$$R(t) = R_p \cdot t^n \quad (2)$$

where $R_p(t)$ is the value of the diameter of the plasma channel as a function of time, R is a constant, and n is an exponent. Values for n can be found in scientific literature (for instance Perez (2007) refers an exponent of 0.29). The distribution of the heat flux inside the plasma channel cannot be considered as uniform. Using spectroscopy Descoedres (2005) and Kojima (2007) found that the temperature is higher in the centre of the channel and a very good fit can be obtained using a Gaussian distribution with an exponent of -4.5 (Ben Salah et al. 2006, Hargrove and Ding 2007), which is in good agreement with measurements obtained using spectroscopy.'

4) Explanation of the data acquisition of discharge voltage in the process of EDM is quite useful to understand this process. However, this manuscript mainly aims to simulate the process of EDM. Please revise the two paragraphs on data acquisition in Section 2, if possible.

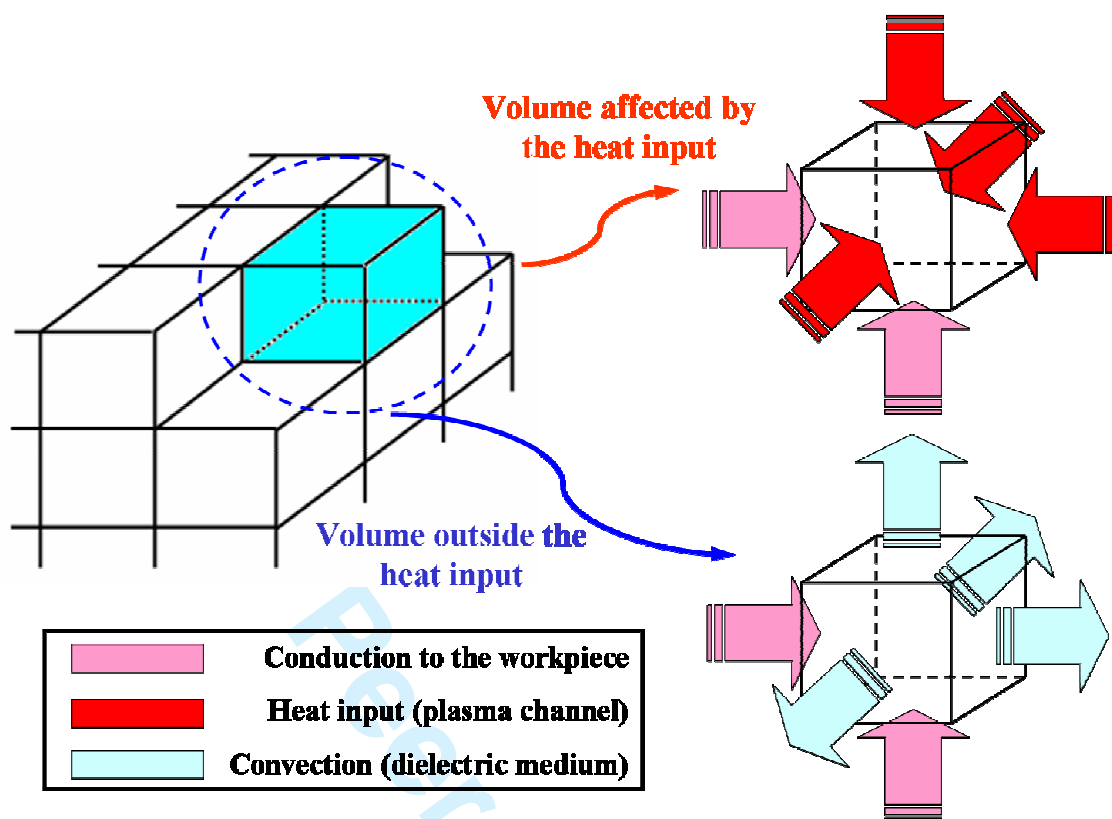
- Both mathematical approach and assumptions considered to develop a certain model are of great importance, but the mathematical accuracy must be accompanied by good input data concerning the process. In this sense it has to take good care when acquiring voltage and intensity data for the model. This is why authors consider that a good definition of the procedure followed in order to acquire data is an interesting topic, so the paragraphs have not been changed.

5) As for Conclusions, the first one is a general statement. It might be better to remove it from the Conclusions.

- The first conclusion has been removed according to this comment.

6) Please check the text in Figure 2. Are both elements inside the plasma channel?

- Two elements are outside the plasma channel, and the others inside it. The figure has been modified to reflect both situations:



- Editors Comments:

1) Please respond to all above.

- All comments have been responded.

2) Consider adding both or just one of the following references at the start of the paper:

- K H Ho and S T Newman 'State of the Art Electro-Discharge Machining', International Journal of Machine Tools & Manufacture, 43(13) pp 1287-1300, 2003.

- K H Ho and S T Newman, S Rahimifard and R D Allen 'State of the Art Wire Electrical Discharge Machining', International Journal of Machine Tools & Manufacture, 44 (12&13), pp 1247-1259, 2004.

- The first of the suggested references has been added since the aim of the present work is to model the SEDM.

3) Reference style incorrect for IJCM, should be named in text and alphabetical order in references list. Please check IJCM website.

- Reference style has been modified.

For Peer Review Only

International Journal of Computer Integrated Manufacturing
Vol. X, No. X, Month 200X, 000–000

International Journal of Computer Integrated Manufacturing

ORIGINAL MANUSCRIPT

Computer simulation of performance of electrical discharge machining operations

For Peer Review Only

International Journal of Computer Integrated Manufacturing
Vol. X, No. X, Month 200X, 000–000

J.A. Sánchez et al.
International Journal of Computer Integrated Manufacturing

ORIGINAL MANUSCRIPT

Computer simulation of performance of electrical discharge machining operations

José Antonio Sánchez^a, Borja Izquierdo^{a*}, Naiara Ortega^a, Iñigo Pombo^a and Itziar Cabanes^a

^a*Department of Mechanical Engineering, Faculty of Engineering of Bilbao, Bilbao, Spain*

Computer simulation of performance of electrical discharge machining operations

José Antonio Sánchez^a, Borja Izquierdo^{a*}, Naiara Ortega^a, Iñigo Pombo^a, Soraya Plaza^a and Itziar Cabanes^b

^a*Department of Mechanical Engineering, Faculty of Engineering of Bilbao, Bilbao, Spain;* ^b*Department of Mechanical Engineering, Faculty of Engineering of Bilbao, Bilbao, Spain*

The Electrical Discharge Machining (EDM) process is optimum for accurate machining of complex geometries in hard materials, as those required in the tooling industry. It has become, by far, the most popular amongst the non-conventional machining processes. However, although a large number of EDM machines are sold every year, available knowledge of the process is still very empirical. Experimental trials are required in many cases to set up the optimum conditions for an EDM operation, resulting in increases in lead-time and cost for the final part. The reason for this is the complex nature of the process, highly stochastic, that involves simultaneous interaction of thermal, mechanical, chemical and electrical phenomena. Therefore, research efforts must be directed towards process modelling in order to reduce the experimental cost associated to the technology. In this work, an original computer simulation model of the EDM process is presented. The model is based on the numerical calculation of temperature fields within the workpiece, from which the amount of part material removed per discharge can be estimated. The objective is to theoretically predict Material Removal Rate (MRR) and the final surface finish of the machined part using as input variables the EDM process parameters and the properties of the work material. The model has been validated by carrying out tests on an industrial EDM machine, showing that it can adequately predict MRR and surface roughness with errors below 9%.

Keywords: electrical discharge machining, simulation, modeling, finite differences method

* Corresponding author. Email: borja.izquierdo@ehu.es

1 State-of-the-Art on simulation of the EDM process

The Electrical Discharge Machining (EDM) process is, by far, the most popular amongst the non-conventional material removal techniques with applications in a broad variety of industries such as die and mould-making, aerospace, automotive, biomedical, micromechanics, etc. The process was initially developed in the 40's by Russian scientists, and since then large industrial and academic efforts have consolidated the technology as a the first option when it comes to the machining of complex geometries in difficult-to-machine materials. Therefore, the EDM process provides an optimum alternative to conventional machining processes such as turning, milling or grinding.

The feature that makes EDM unique with respect to those processes is that the removal mechanism does not involve mechanical contact between tool (electrode) and part. In short, during the EDM process, a series of discrete electrical discharges occur between electrode and workpiece in a dielectric medium (oil or deionised water, depending on the application). The distance between electrode and part is know as the gap (see Figure 1). Thousands of discharges may occur per second. During the application of each discharge local temperature rises at several thousands degrees (probably within the range 10,000 °C – 20,000 °C). As a consequence, part material melts and vaporises (and is removed in the form of debris by dielectric flushing), generating thus craters on the surface of the workpiece. This is the core of the removal process, although scientists still argue on some points of this explanation (Ho and Newman 2003). The resulting surface is well-known by the users of the process because it exhibits a characteristic non-directional pattern.

Although as said before a large number of phenomena occur during the removal process, it is commonly accepted that the most important one is the thermal effect (Van Dijck 1974, Jilani and Pandey 1982, Erden 1983, Singh and Ghosh 1999). Therefore, basic modelling of the EDM process involves placing and solving the heat transmission problem (see Equation 1) assuming a heat input given by each one of the sparks that occur during machining. This equation represents a three dimensional time dependent heat transmission problem involving a heat input. In the mentioned equation k and α are the thermal conductivity of the material being heated and diffusivity respectively and \dot{q}_G represents the value of the heat input. For a given boundary conditions, the solution yields a temperature field from which the amount of part material that melt and vaporises can be predicted.

$$\frac{\partial^2 T}{\partial x^2} + \frac{\partial^2 T}{\partial y^2} + \frac{\partial^2 T}{\partial z^2} + \frac{\dot{q}_G}{k} = \frac{1}{\alpha} \cdot \frac{\partial T}{\partial t} \quad (1)$$

Important research efforts have been carried out to use the above equation for modelling the EDM process. Analytical solutions were proposed in the first years, and still some interesting works can be found using this approach (Jilani and Pandey 1982, Yeo *et al.* 2007). These solutions require less computation time, but the boundary conditions that can be used in these models are more restrictive. A more realistic solution, but to a higher computational cost, can be reached using numerical modelling, using mathematical tools such as the Finite Element Method (Das *et al.* 2003, Schulze *et al.* 2004, Pérez *et al.* 2007, Hargrove and Ding 2007) or the Finite Differences Method (Katz and Tibbles 2005, Ben Salah *et al.* 2006). Simulation of a variant of the EDM process, the so-called Wire EDM technology, has also been addressed in scientific literature (Sanchez *et al.* 2006). No doubt, together with the optimisation of the numerical solution, the biggest challenge is to get a realistic definition of the heat input and the boundary conditions of the problem in order to ensure a good correlation between theoretical predictions and industrial observations.

From a thermal point of view, three aspects must be considered when modelling the heat source:

- The part of the total energy involved in the discharge that is effectively transferred to the workpiece by conduction.
- The geometry of the heat source
- The volume of part material actually removed per discharge by melting and vaporising.

If an energy balance is carried out for a single discharge, it can be observed that part of the energy is dissipated into the surrounding dielectric, part is lost by radiation, and finally, a part is transferred towards both electrode and workpiece by conduction. The part that goes to the workpiece is responsible for material removal in the form of craters and for the global heating of the part material. In an interesting research work, Perez (2001) studied the influence of the thermal properties of different materials on the energy partition, establishing a clear relationship between boiling temperature values and the energy partition ratios, and obtained that the percent of energy transferred to the workpiece (cathode) was 16.7%. Xia (1996) established that convection phenomena can be neglected, and studied the energies distributed into anode and cathode by measuring the temperature raise and removal amount of electrodes. In most of the works found in the scientific literature, the percentage of energy transferred to the workpiece ranges from 14% to 25%.

As far as to the geometry of the heat source concerns, its size and shape have to be simulated. Early analytical models considered a point source, but all the recent models assume that the heat source has a disk shape. Although some authors considered that the shape of the plasma channel remains constant during the discharge, Pandey (1986) obtained an equation to calculate the plasma channel, that grows showing a steep increase in the diameter in the first microseconds of the discharge and a posterior stabilization. It also showed its dependency on material's physical properties. Das (2003), Descoedres (2005), Natsu (2006) and Kojima (2007) made optical observations using high speed framing cameras that corroborate the initial fast growth and later stabilization. This experimental observation is commonly expressed mathematically using Equation 2:

$$R(t) = R_p \cdot t^n \quad (2)$$

where $R_p(t)$ is the value of the diameter of the plasma channel as a function of time, R is a constant, and n is an exponent. Values for n can be found in scientific literature (for instance Perez (2007) refers an exponent of 0.29). The distribution of the heat flux inside the plasma channel cannot be considered as uniform. Using spectroscopy Descoedres (2005) and Kojima (2007) found that the temperature is higher in the centre of the channel and a very good fit can be obtained using a Gaussian distribution with an exponent of -4.5 (Ben Salah *et al.* 2006, Hargrove and Ding 2007), which is in good agreement with measurements obtained using spectroscopy.

The mechanism of material ejection that leads to crater formation must be considered. Although early works considered that all the molten material is effectively removed, experimental observations by Jilani (1982) revealed that under this assumption the values of material removal rate predicted were too high. This fact has also been referred by other authors using single-discharge simulations. Therefore, the concept of *Plasma Flushing Efficiency* can be defined as the fraction of the molten material that is effectively removed from the workpiece. Pérez (2007) has observed that for pulses with duration of 50 μ s and intensity of 5A the crater represents about 35% of the total molten volume. Erden (1983) established that the ejecting efficiency depends on the thermal expansion coefficient of the electrode material, the amount of molten material, the

discharge channel radius, the thermal properties of material and the dielectric flushing conditions. Takezawa (2007) performed a study on single discharge machining with a low melting temperature alloy in order to investigate the material removal mechanism involved in EDM. He found that for long pulses the volume of craters is higher, but its relation with the observed resolidified layer becomes much lower, which is a sign of inefficiency in the material ejection mechanism.

Finally, the problem of discharge location must also be addressed in EDM process modelling. Kunieda studied the main factors determining discharge locations, namely, the distance between electrodes, debris concentration and desionization of previous discharges at every point on the surface that is being eroded (Kunieda and Kiyohara 1998). In this work, Kunieda predicts electrode and workpiece surface after removal, but it does not solve the thermal problem (every discharge removes the same volume of material, according to the measured MRR of the process). Kojima (1992) showed how discharge location is affected by debris concentration within the gap for different flushing conditions.

In this work, a computer simulation model to evaluate the performance of EDM operations is introduced. The thermal models commented before focus on the scientific description of the phenomena involved, based on the analysis of a single spark. This is a good approach to understand the underlying nature of the removal mechanism, but it must be taken into account that single discharges take place in very special conditions, which are different to the actual conditions during practical EDM operations. The model proposed here, based on the thermal description of the problem, considers the superposition of discharges to predict material removal rate and surface topography. The mathematical description of the model is included in Section 2. Discharge location has also been considered in this new model. In order to do so, the dependency of discharge location on the local value of the gap, and on the local presence of debris has been included. Computer numerical simulation has been used to predict local presence of debris. The development of the simulation software is described in Section 3. Once the model is available, its predictions are validated by comparison with industrial EDM operations. Then a study on the influence of the input variables on the accuracy of the model is included in Section 4.

2 Mathematical description of the model

In this work, a first order forward finite difference approach is used to solve the thermal problem. Since it is a 3D problem, hexahedral elements are used in the discretization of the workpiece. For each of these elements the thermal problem must be solved at each time step in the form of finite differences, but it must be taken into account that the boundary conditions are different for each element depending on its location and whether the element is affected by the heat source or not at each time step. On each face of each element, diffusion, convection and/or contribution from the heat source may happen. Figure 2 shows an example of discretization of an irregular surface.

The energy balance in the volume closed by an element is expressed by Equation 3, which includes the effects of conduction, convection, the heat source and the temperature increase in the volume of the element:

$$\sum (\dot{Q}_{IN} - \dot{Q}_{OUT})_{CONDUCTION} - \sum \dot{Q}_{OUT}_{CONVECTION} + \sum \dot{Q}_{IN}_{HEAT_SOURCE} = \dot{Q}_{ACCUMULATED} \quad (3)$$

Each of the terms of Equation 3 can be written in the form of finite differences. Thus, for the term of conduction:

$$\dot{Q}_{CONDUCTION} = -k \cdot \frac{T_{i,j,k,m} - T_{i,j-1,k,m}}{\Delta y} \cdot \Delta x \cdot \Delta z \quad (4)$$

For the boundaries affected by the heat source (q) the general form of the equation is:

$$\dot{Q}_{HEAT_SOURCE} = q \cdot \Delta x \cdot \Delta z \quad (5)$$

For those boundaries where convection applies:

$$Q_{CONVECTION} = h \cdot (T_{i,j,k,m} - T_{\infty}) \cdot \Delta x \cdot \Delta z \quad (6)$$

And finally, for the heat accumulation rate inside the discrete volume during a time step it results:

$$\dot{Q}_{ACCUMULATED} = \frac{\rho \cdot Cp \cdot \Delta x \cdot \Delta y \cdot \Delta z}{k} \cdot \frac{T_{i,j,k,m+1} - T_{i,j,k,m}}{\Delta t} \quad (7)$$

Replacing Equations 4 to 7 in the energy balance, the temperature in each node for the next time step ($T_{i,j,k,m+1}$) can be obtained:

$$T_{i,j,k,m+1} = T_{i,j,k,m} + \frac{k \cdot \Delta t}{\rho \cdot Cp \cdot \Delta x \cdot \Delta y \cdot \Delta z} \cdot \left[-k \cdot \frac{T_{i,j,k,m} - T_{i,j-1,k,m}}{\Delta y} \cdot \Delta x \cdot \Delta z - k \cdot \frac{T_{i,j,k,m} - T_{i,j,k-1,m}}{\Delta z} \cdot \Delta x \cdot \Delta y + q \cdot (\Delta x \cdot \Delta z + \Delta z \cdot \Delta y + 2 \cdot \Delta y \cdot \Delta z) \right] \quad (8)$$

Of course, convergence of the method can only be guaranteed if conditions related to the time step and to the size of the elements are satisfied. The main advantage of this approach is its flexibility to define different boundary conditions virtually for every element, which allows the model to solve the thermal problem even if the heat source is applied over an irregular surface, as it happens during EDM.

Once the basics of the mathematics of the model have been described, the definition of the heat source and the volume of part material removed per discharge can be addressed. The first point is the determination of the total energy developed during the discharge, and the part of that energy that is effectively conveyed to the workpiece. For a given discharge, the energy can be calculated as:

$$E = \int_0^{t_{ON}} U(t) \cdot I(t) \cdot dt \quad (9)$$

where $U(t)$ is the discharge voltage, $I(t)$ the discharge current and t_{on} the discharge duration. In order to obtain a realistic value of the energy, $U(t)$ and $I(t)$ must be measured during an actual EDM operation. To do so, an acquisition system for the capture of current and voltage signals has been implemented. The acquisition hardware has been defined considering the characteristics of the both signals, and involves continuous-time acquisition, sample and storage rate of 5 Msamples/s per channel, two analogue input channels with independent resolution and a minimum input range of 1 V for current signal and 5 V for voltage signal. All these requirements are met by the commercial acquisition board NI-6115 PC board with PCI bus.

Discharge voltage is transmitted to the data acquisition board using a low voltage shielded cable. Discharge voltage is obtained by a voltage divider so as not to exceed the board input range. Discharge current is taken from the discharge circuit. Discharge current is converted to voltage through a Tektronix current probe. Both signals are transferred to the BNC-2110 Noise-Rejecting BNC I/O Connector Block, which is attached to NI-6115 data acquisition board through SH68-68-EP Noise-Rejecting Shielded Cable. Each BNC connector placed in the BNC Adapter is provided with a two-position switch: Floating Source (FS) and Ground-referenced Source (GS). As its label points out, FS is selected when measuring floating signal sources. In this case, the amplifier negative terminal connects to ground through a 5 k Ω resistor in parallel with a 0.1 μ F capacitor. This resistor provides a return path for the ± 200 pA bias current. Otherwise, the floating source is not likely to remain within the common-mode signal range of the PGIA. Consequently, the PGIA saturates, causing erroneous readings. As GS is concerned, it is selected when measuring ground-referenced sources for avoiding ground loops. The acquisition system PC is a 3.6 GHz Pentium IV provided with 300 GB storing space hard disk and 2 GB of RAM memory. Since the file system is NTFS, the file size limit to be stored continuously depends mainly on the hard disk capacity. In the specific case of wire breakage in WEDM, the duration of a test continuously acquired can last from 4 to 60 minutes, which corresponds to around 5 and 75 GB respectively. The high speed libraries of the LabviewTM graphical programming language have been used for the development of applications aimed at exploiting the acquisition system hardware.

Since the acquisition is continuous, a circular buffer is used. Hence, while the buffer is filled with the data from the NI-6115 board, another block of data is retrieved from the buffer. When the end of the buffer is achieved, the acquisition system returns to the beginning and continues filling the same buffer. When the data is overwritten before being retrieved, an error is generated. In order to avoid this error, two parameters have been adjusted: the buffer size and the number of scans to store to disk at a time. Before executing the software, the user has to fill in four fields. The first field is the number of device assigned to NI-6115 acquisition board. Secondly, the user has to introduce the names of the virtual channels. A virtual channel is a shortcut to a pre-configured analogue input channel of the NI-6115. Every time a virtual channel is called, the respective analogue input adopts the preconfigured characteristics such as the gain and the grounding mode. Both the number of device and the virtual channels can be configured from a National Instruments software interface called Measurement & Automation Explorer.

Following the literature review (see Section 1) it can be assumed that a constant fraction of the energy of the discharge is transferred to the workpiece by conduction (Q_w). The heat source is modelled using a circular geometry and the heat flux inside the plasma channel is described using a Gaussian distribution. The elements outside will be affected by convection of the dielectric around the workpiece. The dependency of the plasma channel radius with time is expressed using Equation 2.

With these inputs the model can be mathematically solved using Equations 3 to 8. The result is the temperature distribution inside the workpiece due to the discharge. At this point, a criterion for material removal must be defined: every element on the workpiece that has reached a temperature higher than the so-called *equivalent temperature* (T_{eq}) is removed. When material disappears a new crater is generated on the surface. Thus, some elements inside the bulk material may now become the free surface of the workpiece. Therefore, the boundary conditions vary from one time step to the next, and this important fact is considered by the proposed model.

The effect of establishing different values of T_{eq} on the geometry of the generated crater is shown in Figure 4. The figure represents a plane section of the three dimensional temperature distribution inside the workpiece due to a discharge. The isotherms corresponding to equivalent temperatures of 1500, 2500 and 3200 have been represented. Obviously, the material removed in each case varies largely, with differences in volume that can reach up to 80%. It can be seen that the model must solve the thermal problem when the heat input is applied on an irregular surface like the one that characterizes the EDM process.

The definition of discharge location has also been included in the model. A probability function has been obtained so that for points whose distance to the electrode is short (peaks on the eroded surface) discharge probability is higher than that for points further from the electrode (valleys of the EDM-ed surface) (Kojima *et al.* 1992, Kunieda and Kiyohara 1998). This probability function is used to determine the element of the discretized surface on which the next discharge will take place. The mentioned function has been obtained from experimental results obtained in discharge test carried out on stepped workpieces. The aim of these tests was to count the number of discharges occurred in the top surface and in the lower surface of the stepped piece for different step heights. It was observed that as the step height increases the probability of discharge occurrence on the top surface tends to be 100%, while for low step heights it tends to be equally distributed (50% of spark occurrence in both low and top surfaces). Empirical results obtained with these tests were included in the model, in such a way that points of the eroded surface located closer to the electrode (peaks of the surface) have greater probability for discharges to take place on them.

Even though at the current stage of modelling the influence of debris concentration on discharge location is not included in the model yet, a preliminary study has been carried out. First, the velocity field produced by a jet of dielectric flushing between the flat surfaces of both electrode and workpiece has been numerically calculated using Computational Fluid Dynamics (CFD). The results of the simulation, shown in Figure 5, reveal higher velocities at the centre of the workpiece. Therefore, it can be assumed that debris produced by the EDM process will be removed from that zone. At the sides, where lower velocities are predicted, debris will tend to accumulate.

EDM experiments have been carried out under similar flushing conditions to those imposed on the above numerical simulation. The EDM'ed surfaces have been measured using a contact profilometer (see section 4 for more details). The results, shown in Figure 6, reveal that more workpiece material is removed at the centre of the workpiece, where dielectric velocity is higher and therefore debris is more easily removed by the dielectric flushing. It can be concluded that important information can be extracted from CFD to include the effect of debris concentration in the model. As it has been said, the aim of CFD simulations was to show that debris concentration influences discharge characteristics, so discharges which take place in clean dielectric lead to different material removal rates and surface finishes than those discharges affected by high concentrations of debris. However, representing the effect of debris on EDM in a modelling of the process is very difficult. For that reason the validation of the present model has been performed on the hypothesis that

the dielectric medium is clean. Tests carried out for the validation have been done under optimum flushing conditions taking special care to guarantee that the dielectric is clean in all the working area, and in the modelling tool it has been assumed that debris concentration is the same in all the points of the simulated surface.

3 Development of the simulation software

The sequence of events during simulation is presented in Figure 7, and is the basis for the computer simulation software. The software has been programmed in C++ programming language using the environment provided by Borland C++ Builder. C++ supports Object-Oriented Programming (OOP). This means that uses objects and interactions between them to design application such as simulation software like the one described here. Features and concepts such as modularity, classes, objects, etc. are typical of this programming concept.

The software has been divided into different modules and classes in order to achieve an easy-to-maintain final code. Memory management has been probably one of the most difficult problems due to the huge amount of data required to simulate the actual dimensions of the workpiece. The following solutions have been considered:

- Working with advanced memory management in Windows. This option has been discarded due to the difficulties found in the portability of the code from one platform to another.
- Working with a file found in the hard disk, but keeping independent tasks for loading data and saving calculated data in the hard disk. Calculations are performed in temporal matrices generated in the memory, and once the mathematical operation is finished, the obtained values are saved in the file on the hard disk. This has been the selected option: portability of the code is assured, and with the use of *threads* and multi-core processors, simulation time can be greatly reduced.

In order to avoid loss of information and at the same time, make an optimal use of the available memory, a real type matrix of simple precision has been used to store temperature data in milligrades (10^{-3} °C). However, in the function in which calculations are performed, double precision has been specified to avoid truncation that can lead to important errors. Improvements in the use of the memory relating the properties of each node have also been achieved. Instead of using a 3-dimensional matrix to store the types and the properties of the nodes, a 2-dimensional matrix for each column that represents the workpiece has been defined.

Post-processing capabilities have been installed in the software in order to make easier the analysis of the results. As well as values of surface finish, material removal rates and temperature fields, the user will have the possibility of obtaining the sub-surface metallurgical changes that can occur inside the workpiece as a consequence of the EDM process. OpenGL is the tool selected for the graphic interface and display of the results.

Finally it must be mentioned that, although at the current stage of the work the software has been programmed in Borland C++, the first steps towards the implementation of the code using QT4 for the design of the forms have been given.

4 Industrial validation of the software

Results obtained from simulations have been compared with EDM tests carried out on an ONA H300 industrial EDM machine. The material for the tests is AISI D2 tool steel, commonly used in EDM operations for tool manufacturing. Thermo-physical properties of the material, variable with temperature, are listed in Table 1. Both electrode and workpiece have square section with side length 30mm. EDM conditions have been selected by machine table look-up, and they are collected in Table 2.

Validation of the model involves comparing the machining performance predicted by the software with that of an actual EDM industrial operation in terms of surface finish and material removal rate. Due to the stochastic nature of the EDM'ed surfaces, amplitude parameters such as S_a (average roughness), S_q (root mean square of height distribution) and S_z (average difference between the 5 highest peaks and the 5 lowest valleys) may not be enough to adequately describe the obtained surface finish. Therefore, it was decided to include also hybrid parameters such as S_{dq} (root mean square of the topographic surface) and S_{dr} (developed interfacial area ratio), which are useful to distinguish surfaces with the same S_a . Figure 8 illustrates this fact, showing that surfaces with similar value of S_a may exhibit very different values of S_{dq} .

It must be taken into account that surface roughness parameters are defined statistically. The formulae for the calculus of these parameters are given below:

$$S_a = \frac{1}{MN} \sum_{k=0}^{M-1} \sum_{l=0}^{N-1} |Z(x_k, y_l) - \mu| \quad (10)$$

Where μ is the mean height of the profile:

$$\mu = \frac{1}{MN} \sum_{k=0}^{M-1} \sum_{l=0}^{N-1} Z(x_k, y_l) \quad (11)$$

And the equation for S_{dq} is:

$$S_{dq} = \sqrt{\frac{1}{(M-1)(N-1)} \sum_{k=0}^{M-1} \sum_{l=0}^{N-1} \left(\frac{Z(x_k, y_l) - Z(x_{k-1}, y_l)}{\Delta x} \right)^2 + \left(\frac{Z(x_k, y_l) - Z(x_k, y_{l-1})}{\Delta y} \right)^2} \quad (12)$$

This means that two different surfaces that exhibit similar values of amplitude parameters (such as S_a , S_q and S_z) may produce different values of hybrid parameters (such as S_{dq} and S_{dr}). Of course, this is independent on the manufacturing process used to generate the surface. In other words, this is not an intrinsic property of EDM-ed surfaces.

As far as to the surfaces represented in Figure 9 refers, the one at the right has been generated using a low value of the plasma radius (input variable R_p) that produces small craters, whilst the one at the left has been generated using a higher value of R_p . The result is two different surfaces that exhibit similar values of S_a , but different values of S_{dq} .

The experimental determination of these surface parameters of EDM-ed surfaces was performed with a contact profilometer (Taylor Hobson Talysurf Series 2) and with surface analysis software associated to the

profilometer (TalyMap Expert 3.1.9). This software was also employed to analyse results of the simulations. Since the model generates surfaces of 1.2x1.2mm, experimental measurements have been performed in areas with the same size as simulated surfaces. Four measurements were carried out, each of them in a different location of the 30x30mm eroded surface and their mean value was used to compare experimental and simulated surfaces.

In order to quantify the deviation in the prediction of the surface finish, an error function is defined as:

$$E_s = \sqrt{\frac{\left(\frac{Sa_s - Sa_e}{Sa_e}\right)^2 + \left(\frac{Sq_s - Sq_e}{Sq_e}\right)^2 + \left(\frac{Sz_s - Sz_e}{Sz_e}\right)^2 + \left(\frac{Sdq_s - Sdq_e}{Sdq_e}\right)^2 + \left(\frac{Sdz_s - Sdz_e}{Sdz_e}\right)^2}{5}} \quad (14)$$

where the subscript s refers to the simulated and e to the experimental results.

Figure 10 and Table 3 show the results corresponding to an example of validation of the software. At a first view, the topography of simulated and EDM'ed surfaces are very similar. In fact, measurements show an excellent agreement of simulated results with experimental results, the error in the prediction of surface finish being below 9%, and the error in the prediction of material removal rate being as low as 1.96%.

The present model aims to be general, and suitable for both roughing and finishing conditions. Although this work is still in progress additional simulations have been carried out for another regime, different to the one mentioned above. Electrical parameters for this regime are listed in Table 4 and the results of the comparison between predicted and experimental material removal rates and roughness parameters are shown in Table 5. As for the other studied regime, the error in the predicted material removal rate is very low (< 1%), while the error for the considered roughness parameters is lower than 10% except for S_{dr} . In this case the error is slightly higher, with a value of 13.78%, which still represents a good approximation.

At the sight of these results it can be concluded that the model is able to optimally predict the performance of industrial Electrical Discharge Machining operations.

5 Analysis of the influence of the input variables on the accuracy of the model

As commented in the review of the State-of-the-Art, the model is governed by the variables that define the partition of the discharge energy (Q_w), the geometry of the heat source (R_p), and the volume of part material actually removed per discharge by melting and vaporising (T_{eq}). In the validation of the model, data extracted from literature have been used to establish the values of the considered input variables before performing simulations. Results of simulations have been compared with experimental machining tests to validate the proposed model (as explained in section 4). However, these data correspond to a given EDM regime, and therefore will vary for other regimes. In order to evaluate the influence of these inputs on the accuracy of the model a systematic study was carried out. A two-level, four-factor full factorial experiment design was chosen. The factors are Q_w , T_{eq} , R_p and the exponent of the Gaussian heat flux distribution, and for each combination of input parameters three simulations were made, to consider the stochastic nature of their results. Table 6 shows the performed simulations and their results expressed using the mean value of the three simulations carried out for every parameter combination:

Results from simulations were analysed using ANOVA. The percentage of contribution of each factor in the variance of the response variables can be obtained from the sums of squares given by the ANOVA.

These contribution proportions are shown in Figures 10, 11 and 12, and are representative of the importance of each factor. It can be observed that, except for S_{dq} and S_{dr} , the contribution of the error in the ANOVA tests is high (21-38%), which in fact reflects the stochastic nature of the EDM'ed surfaces. Actually, if several roughness measurements are carried out on a part machined in an industrial EDM operation, the same variability is observed. This aspect must be taken into account when considering the contribution of the different input variables on the response.

Figure 11 shows the contribution of the studied factors to S_a and S_z . The error factor has a contribution percent higher than 30%, but despite this fact an underlying effect of Q_w , T_{eq} and R_p can be observed. It can also be concluded that the less important factor affecting S_a and S_z is the exponent of the Gaussian function defining the heat flux

The contribution percents of the inputs on S_{dq} and S_{dr} have a different pattern compared to the ones shown in Figure 12. In this case it is clear that the most influencing factor is R_p , while Q_w and T_{eq} have no influence on these surface parameters.

Finally, the contribution of the studied factors to material removal rate can be seen in Figure 13. In this case R_p and the exponent of the Gaussian function do not seem to affect the prediction of material removal rate, while Q_w and T_{eq} have an important influence. Moreover, from all these results it can be concluded that the exponent of the Gaussian is the factor with less influence among the four inputs considered in this study.

From the above results interesting conclusions can be drawn. On the one hand, the input values of T_{eq} , Q_w and R_p are responsible for important differences in the accuracy of the model and therefore their values must be set for any different EDM regime, [this is, for other machining parameters or materials](#). On the other, the exponent of the Gaussian distribution has a negligible influence on the accuracy of the model, and therefore its value can be set at -4.5 as recommended by other authors in the literature.

6 Conclusions

In this paper an original computer numerical model for the prediction of the performance of EDM operations is presented. From the work carried out, the following conditions can be drawn:

- The mathematics of an original numerical model for simulation of the EDM process have been presented. The model generates EDM'ed surfaces by calculating temperature fields inside the workpiece using a finite difference-based approach, and taking into account the effect of successive discharges.
- The model has been implemented on a computer simulation software. OOP programming has been used, and efficient memory management techniques have been implemented. Post-processing capabilities have been installed in the software in order to make easier the analysis of the results. The user has access to information such as prediction of material removal rate, surface finish, and in a later stage of development, subsurface metallurgical changes due to the EDM process.
- Validation of the model has been carried out by comparing simulated results and those corresponding to an industrial EDM operation. Results show an excellent agreement, with

deviations below 9% in the prediction of surface finish, and as low as 1.96% in the prediction of material removal rate.

- The influence of the parameters that govern the model, namely R_p , T_{eq} and Q_w , has been analysed using the systematic approach provided by ANOVA techniques. Results show that material removal rate is mainly influenced by Q_w and T_{eq} , whereas the higher influence on surface finish is due to R_p . It has also been concluded that the influence of the exponent of the Gaussian distribution can be neglected.

7 Acknowledgements

The authors wish to thank the Spanish Ministry of Education (MEC) for their support to the Research Project “An original numerical model for the simulation of material removal, electrode wear and surface integrity in the Electrical Discharge Machining (EDM) process”, DPI2007-60143.

8 Bibliography

- Ben Salah, N., Ghanem, F. and Ben Atig K., 2006. Numerical Study of thermal aspects of electric discharge machining process. *Int. J. of Machine Tools and Manufacture*, 46, 908-911.
- Das, S., Klotz, M. and Klocke F., 2003. EDM simulation: finite element-based calculation of deformation, microstructure and residual stresses. *J. of Materials Processing Technology*, 142, 434-451.
- Descocudres, A., Hellenstein, Ch., Walder, G. and Perez R., 2005. Time-resolved imaging and spatially-resolved spectroscopy of electrical discharge machining plasma. *J. of Applied Physics*, 38, 4066-4073.
- Erden, A., 1983. Effect of Materials on the Mechanism of Electric Discharge Machining (EDM). *Transactions of the ASME*, 105, 132-138.
- Hargrove, S. K. and Ding, D., 2007. Determining cutting parameters in wire EDM based on workpiece surface temperature distribution. *Int. J. Advanced Manufacturing Technologies*, 34, 295-299.
- Ho, K.H., and Newman, S. T., 2003. State of the Art Electro-Discharge Machining. *International Journal of Machine Tools & Manufacture*, 43 (13), 1287-1300.
- Jilani, S.T. and Pandey, P.C., 1982. Analysis and modelling of EDM parameters. *Precis. Eng.*, 4 (4), 215–221.
- Katz, Z. and Tibbles C.J., 2005. Analysis of micro-scale EDM process. *Int. J. Advanced Manufacturing Technologies*, 25, 923–928.
- Kojima, H., Kunieda, M. and Nishiwaki, N., 1992. Understanding Discharge Location Movements during EDM. *10th International Symposium for Electromachining, ISEM X*, 144.
- Kojima, A., Natsu, W. and Kunieda M., 2007. Observation of Arc Plasma Expansion and Delayed Growth of Discharge Crater in EDM. *Proceedings of the 15th International Symposium on Electromachining, ISEM XV*, 1–4.

- Kunieda, M. and Kiyohara M., 1998. Simulation of Die-Sinking EDM by Discharge Location searching Algorithm. *Int. J. of Electrical Machining*, 79-85.
- Natsu, W., Shimoyamada, M. and Kunieda M., 2006. Study on Expansion Process of EDM Arc Plasma. *JSME International Journal*, Series C, Vol. 49, No. 2, 600-605.
- Pandey, P.C. and Jilani, S.T., 1986. Plasma channel growth and the resolidified layer in EDM. *Precis. Eng.*, 8 (2), 104–110.
- Pérez, R., Chiriotti, N., Demellayer, R., Flükiger, R. and Zryd A., 2001. Investigation of physical processes in wire-EDM by means of single and multiple discharge measurements and análisis. *13th International Symposium for Electromachining, ISEM XIII*, Vol. II, 701-715.
- Pérez, R., Carron, J., Rappaz, M., Wälder, G., Revaz, B. and Flükiger, R., 2007. Measurement and Metallurgical Modelling of the Thermal Impact of EDM Discharges on Steel. *Proceedings of the 15th International Symposium on Electromachining, ISEM XV*, 17–22.
- Sanchez, J.A., Plaza, S., Lopez de Lacalle, L.N. and Lamikiz, A., 2006. Computer simulation of wire EDM taper-cutting. *Int. J. of Computer Integrated Manufacturing*, Vol. 19 (7), 727-735.
- Singh, A. and Ghosh, A., 1999. A thermo-electric model of material removal during electric discharge machining. *Int. J. of Machine Tools & Manufacture*, 39, 669-682.
- Schulze, H.P., Herms, R., Juhr, H., Schaetzing, W. and Wollenberg, G., 2004. Comparison of Measured and Simulated crater morphology for EDM. *J. of Materials Processing Technology*, 149, 316-322.
- Takezawa, H., Kokubo, H., Mohri, N., Horio, K., Yanagida, D. and Saito N., 2007. A Study on Single Discharge Machining with Low Melting Temperature Alloy, *Proceedings of the 15th International Symposium on Electromachining, ISEM XV*, 69–73.
- Van Dijck, F., 1973. *Physico-mathematical analysis of the electr discharge machining process*. Thesis (PhD) (English translation). Catholic-University of Leuven.
- Xia, H., Kunieda, M. and Nishiwaki N., 1996. Removal Amount Difference between Anode and Cathode in EDM Process. *Int. J. of Electrical Machining*, 1, 45-52.
- Yeo, S.H., Kurnia, W. and Tan P.C., 2007. Electro-thermal modelling of anode and cathode in micro-EDM, *Journal of Physics Applied Physics*, 40, 2513–2521.

Table 1 AISI D2 tool steel thermal properties.				
AISI D2 tool steel				
T [°C]	K [W/(m·°C)]	ρ [kg/m ³]	c_p [J/(kg·1C)]	α [m ² /s]
30	19.79	7740	461.05	$5.55 \cdot 10^{-6}$
200	21.95	7740	541.4	$5.24 \cdot 10^{-1}$
400	24.5	7740	635.9	$4.98 \cdot 10^{-6}$
600	27.03	7740	730.4	$4.78 \cdot 10^{-6}$

Table 2 EDM conditions used for experimental tests (first erosion regime).	
EDM conditions	
On-time (t_{on})	50 μ s
Off-time (t_{off})	13 μ s
Open-circuit voltage (U_0)	200V
Gap servo voltage (V_{gap})	25V
Discharge current (I)	8A
Electrode material	Copper
Dielectric fluid	EDM fluid GR2 (by Steelfluid)
Flushing	External

Table 3 Comparison between simulated and measured surfaces for the first studied regime.											
	Q_w	T_{eq} [°C]	R_p	S_a [μ m]	S_q [μ m]	S_z [μ m]	S_{dq} [μ m/ μ m]	S_{dr} [%]	E_s	MRR [mm ³ /min]	Error MRR [%]
SIMULATION	0.21	1963	626	7.33	9.28	61.7	0.475	10.7	0.00935	46.9	1.96
EXPERIMENTAL	-	-	-	7.26	8.98	60.4	0.48	10.65	-	46	-

Table 4 EDM conditions used for experimental tests (second erosion regime).	
EDM conditions	
On-time (t_{on})	18.2 μ s
Off-time (t_{off})	6.5 μ s
Open-circuit voltage (U_0)	200V
Gap servo voltage (V_{gap})	25V
Discharge current (I)	6A
Electrode material	Copper
Dielectric fluid	EDM fluid GR2 (by Steelfluid)
Flushing	External

Table 5 Comparison between simulated and measured surfaces for the second regime.											
	Q_w	T_{eq} [°C]	R_p	S_a [μ m]	S_q [μ m]	S_z [μ m]	S_{dq} [μ m/ μ m]	S_{dr} [%]	E_s	MRR [mm ³ /min]	Error MRR [%]
SIMULATION	0.075	2000	502	3.073	3.84	24.21	0.362	6.44	0.0411	4.5	0.24
EXPERIMENTAL	-	-	-	3.33	4.215	26.35	0.344	5.66	-	4.52	-

Table 6 Two-level four-factor full factorial experiment design and results of simulations										
Number of simulation	Q_w	T_{eq} [°C]	R_p	Gaussian exponent	S_a [μ m]	S_q [μ m]	S_z [μ m]	S_{dq} [μ m/ μ m]	S_{dr} [%]	MRR [mm ³ /min]
1	20	1600	500	-3	8.67	10.87	69.87	0.53	13.03	141.8
2	20	1600	1000	-3	7.7	9.62	57.87	0.33	5.39	100.69
3	20	1600	500	-6	8.72	10.83	68.53	0.62	17.63	116.13
4	20	1600	1000	-6	8.28	10.37	63.3	0.42	8.38	141.8

5	20	2500	500	-3	8.14	10.09	62.2	0.51	12.33	93.32
6	20	2500	1000	-3	3.77	4.74	24.43	0.23	2.57	20.28
7	20	2500	500	-6	8.42	10.5	69.83	0.62	18.03	84.68
8	20	2500	1000	-6	7.31	9.13	56.9	0.4	7.62	70.46
9	35	1600	500	-3	10.28	12.8	78.97	0.57	15.27	209.55
10	35	1600	1000	-3	8.25	10.36	61.53	0.33	5.4	251.27
11	35	1600	500	-6	9.53	11.77	74.6	0.63	18.6	160.91
12	35	1600	1000	-6	9.51	11.87	70.23	0.44	9.21	250.49
13	35	2500	500	-3	8.92	11.27	71.8	0.53	13.27	152.81
14	35	2500	1000	-3	7.71	9.6	57.17	0.33	5.27	122.49
15	35	2500	500	-6	9.02	11.2	74.83	0.63	18.63	123.49
16	35	2500	1000	-6	8.58	10.72	66.23	0.42	8.59	158.94

Figure 1. Removal mechanism during the EDM process.

Figure 2 Example of hexahedral element and its boundary conditions.

Figure 3. Block diagram of the acquisition system.

Figure 4. Temperature distribution, isotherms and crater shape for equivalent temperatures of 1500, 2500 and 3200 °C.

Figure 5. CFD simulation results.

Figure 6. Surface measured with contact profilometer.

Figure 7. Algorithm for numerical simulation.

Figure 8. Simulations with similar values of S_a and different values of S_dq .

Figure 9. Example of surfaces showing similar S_a but different S_dq values.

Figure 10. Topography of simulated and measured surfaces.

Figure 11. Contribution percents on S_a and S_z .

Figure 12. Contribution percents on S_dq and S_dr .

Figure 13. Contribution percents on material removal rate.

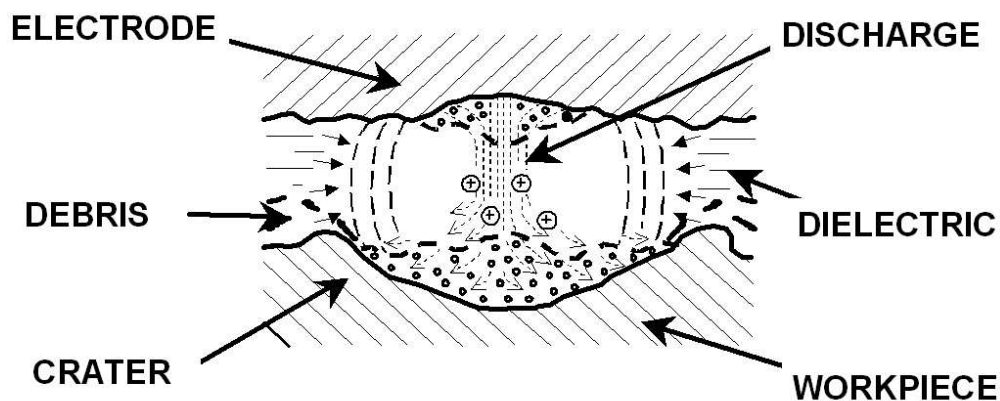


Figure 1. Removal mechanism during the EDM process.
270x118mm (96 x 96 DPI)

er Review Only

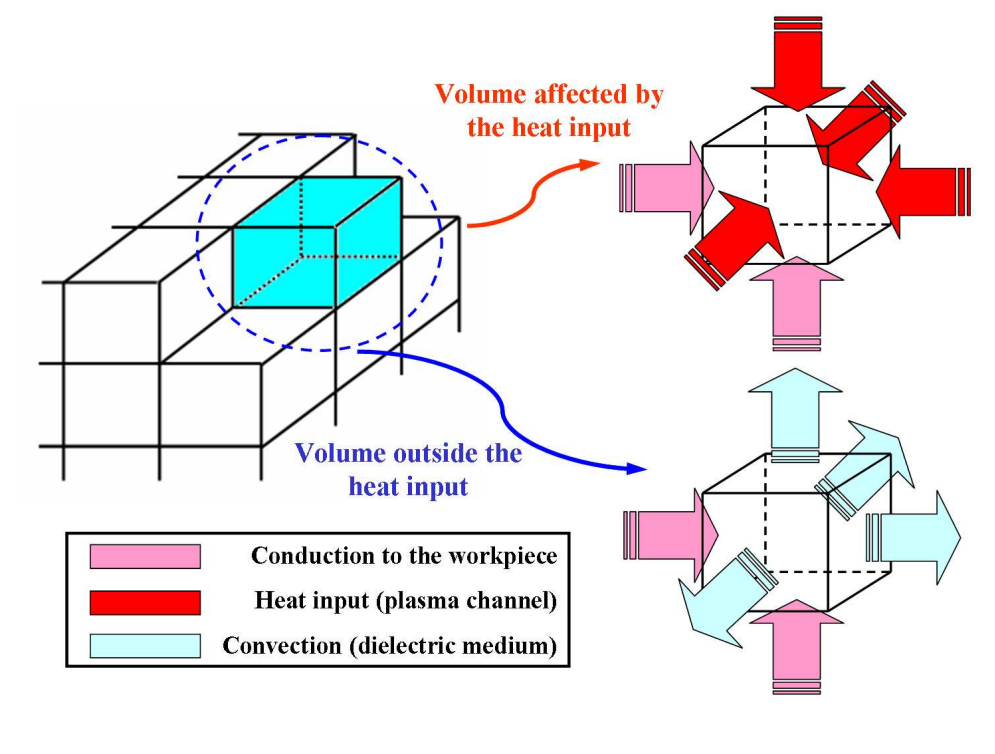


Figure 2 Example of hexahedral element and its boundary conditions.
254x190mm (150 x 150 DPI)

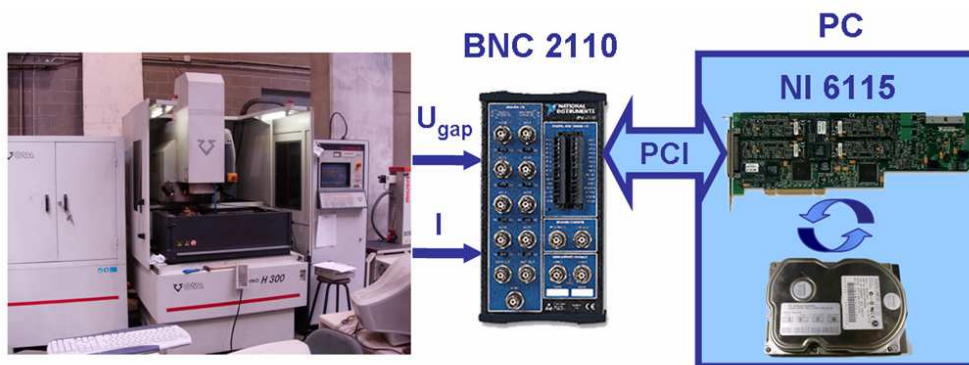


Figure 3. Block diagram of the acquisition system.
270x109mm (96 x 96 DPI)

Pre-Review Only

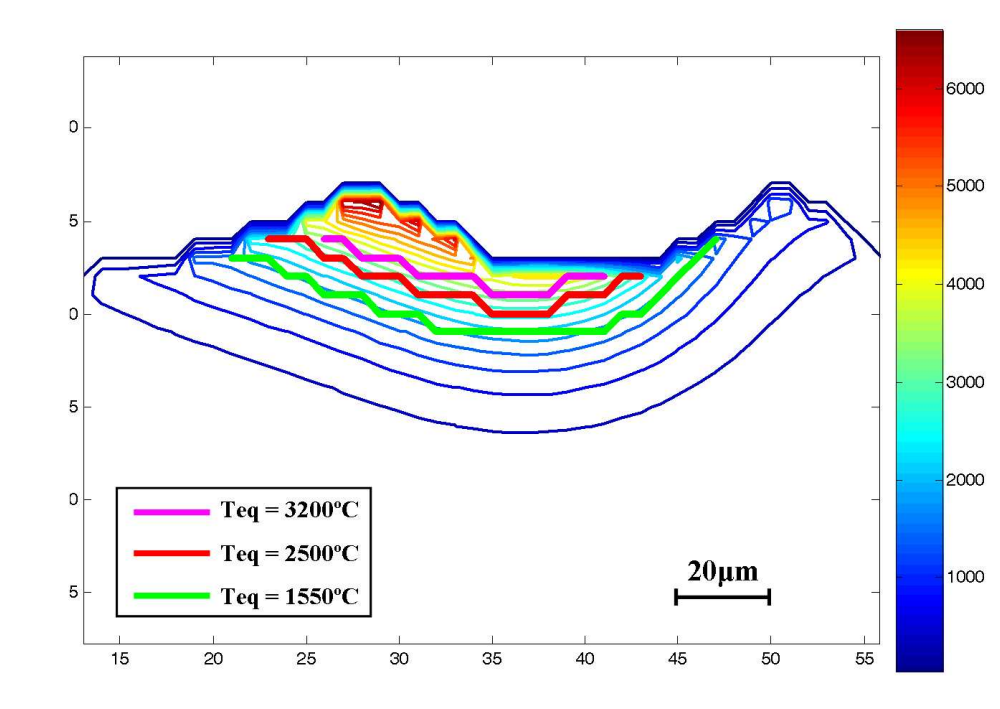


Figure 4. Temperature distribution, isotherms and crater shape for equivalent temperatures of 1500, 2500 and 3200 μC .
236x166mm (150 x 150 DPI)

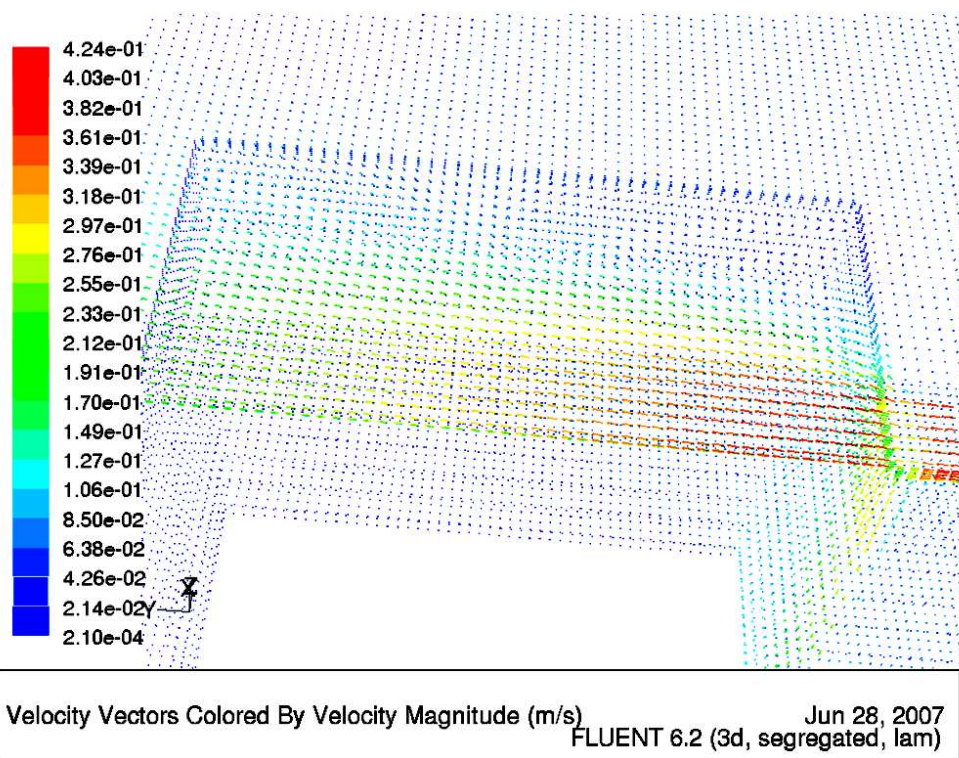


Figure 5. CFD simulation results.
270x203mm (96 x 96 DPI)

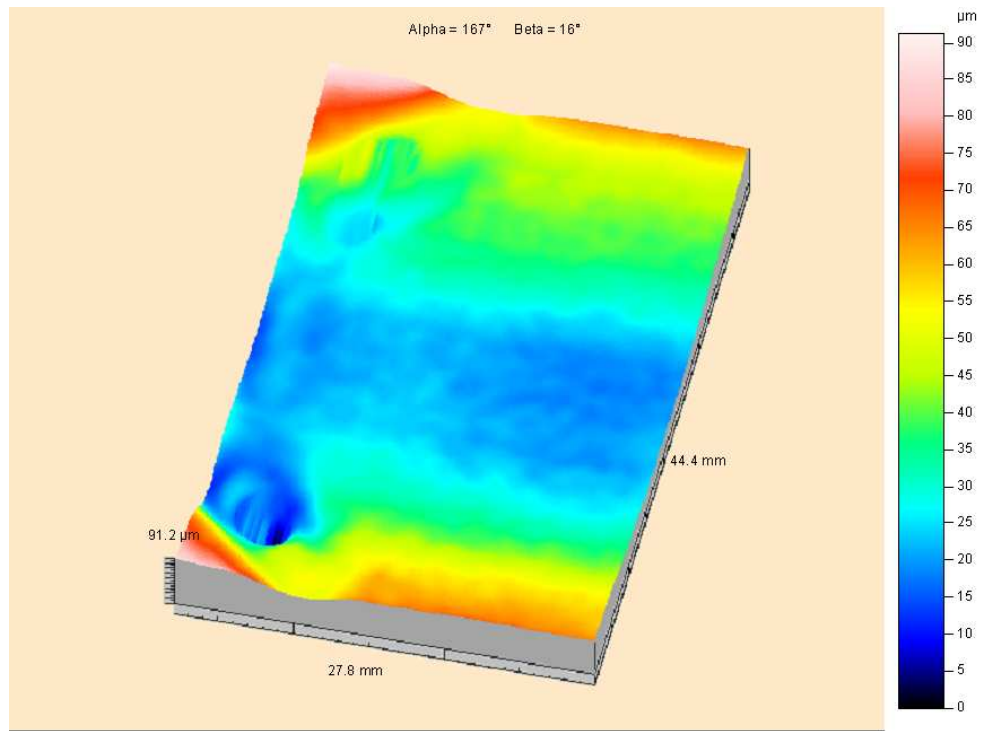


Figure 6. Surface measured with contact profilometer.
150x109mm (150 x 150 DPI)

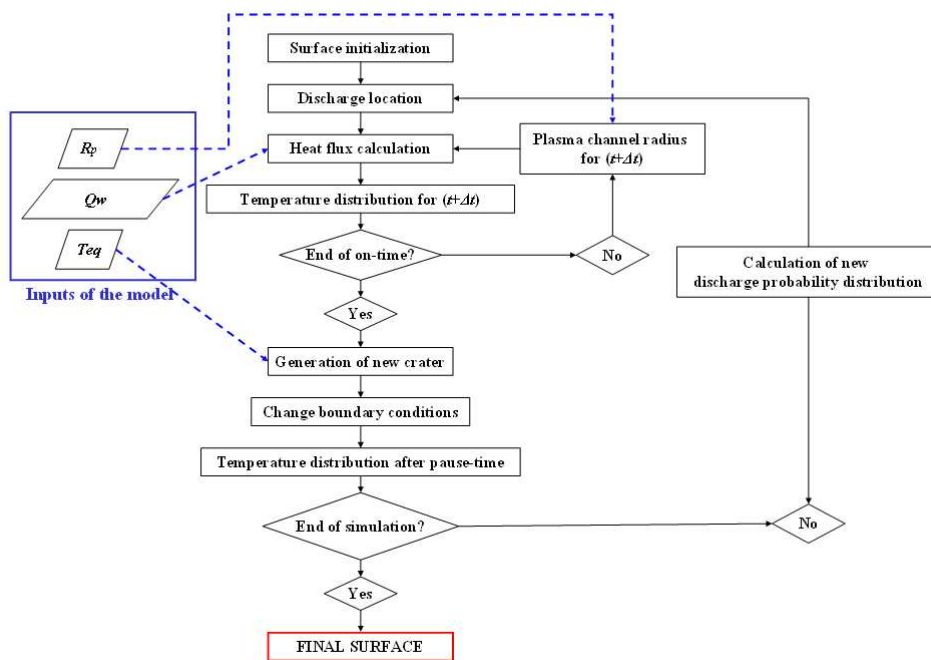


Figure 7. Algorithm for numerical simulation.
264x182mm (96 x 96 DPI)

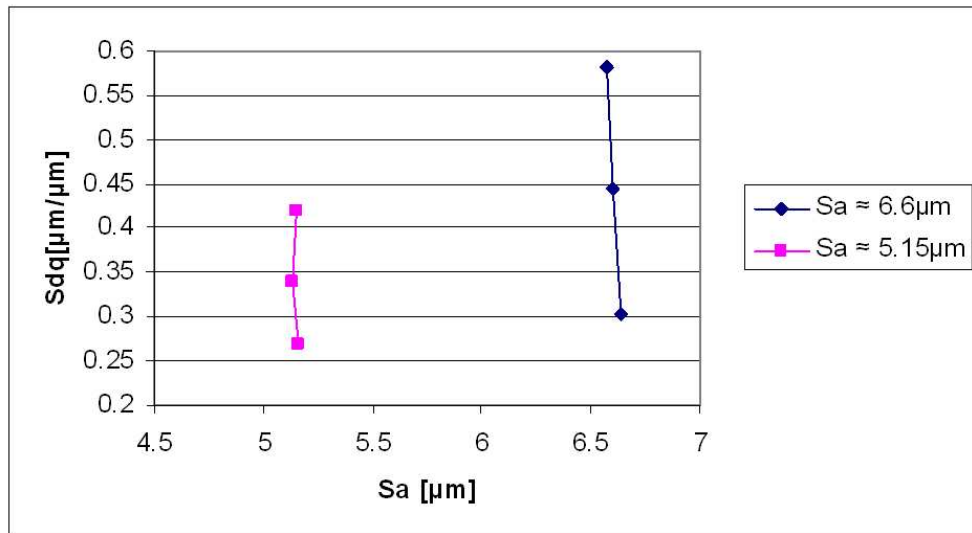


Figure 8. Simulations with similar values of Sa and different values of Sdq.
252x142mm (96 x 96 DPI)

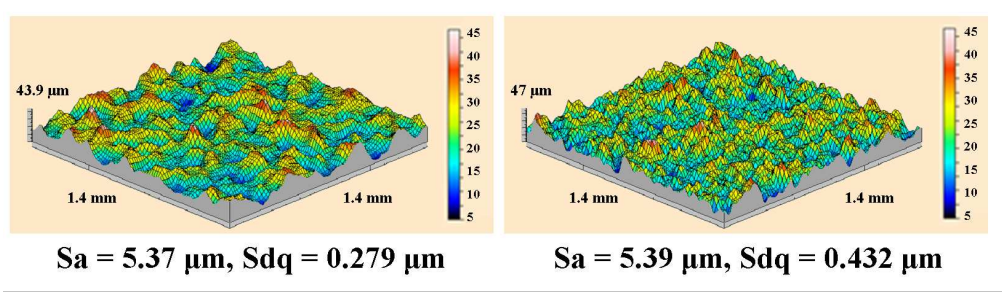


Figure 9. Example of surfaces showing similar Sa but different Sdq values.
275x80mm (150 x 150 DPI)

Peer Review Only

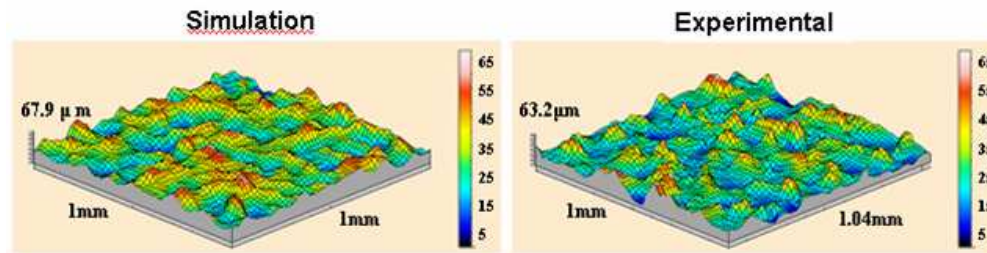


Figure 10. Topography of simulated and measured surfaces.
231x61mm (70 x 70 DPI)

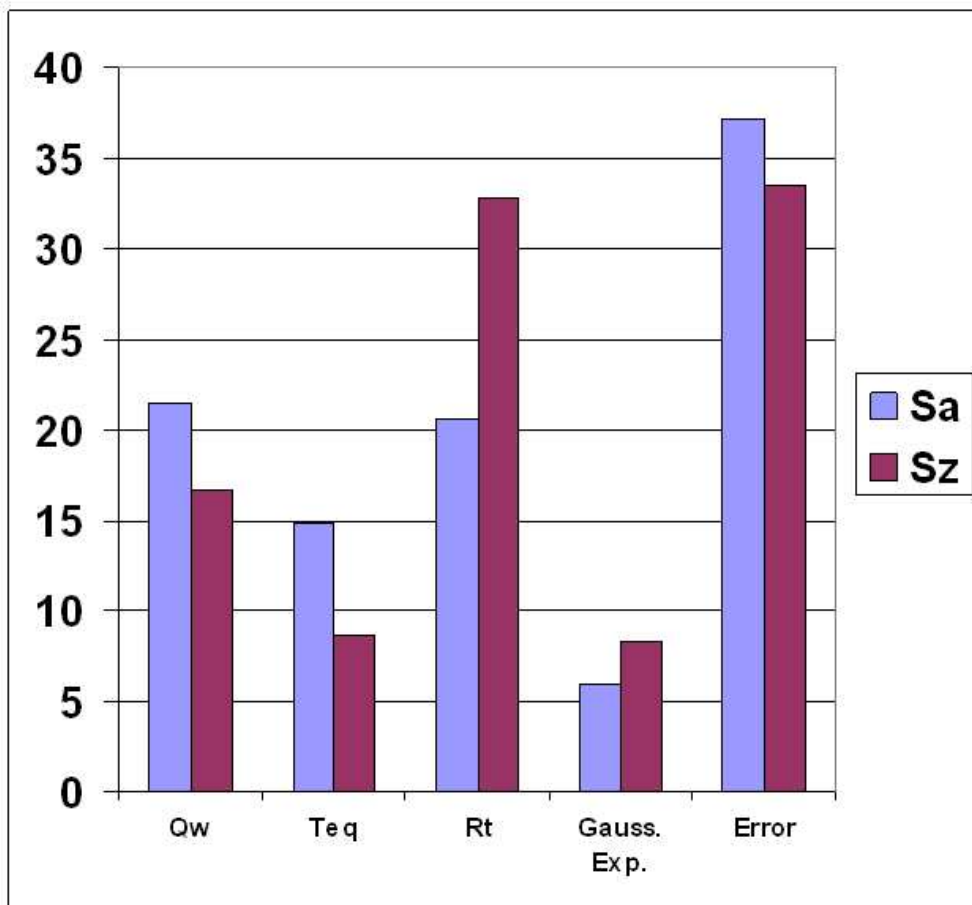


Figure 11. Contribution percents on Sa and Sz.
167x155mm (96 x 96 DPI)

Only

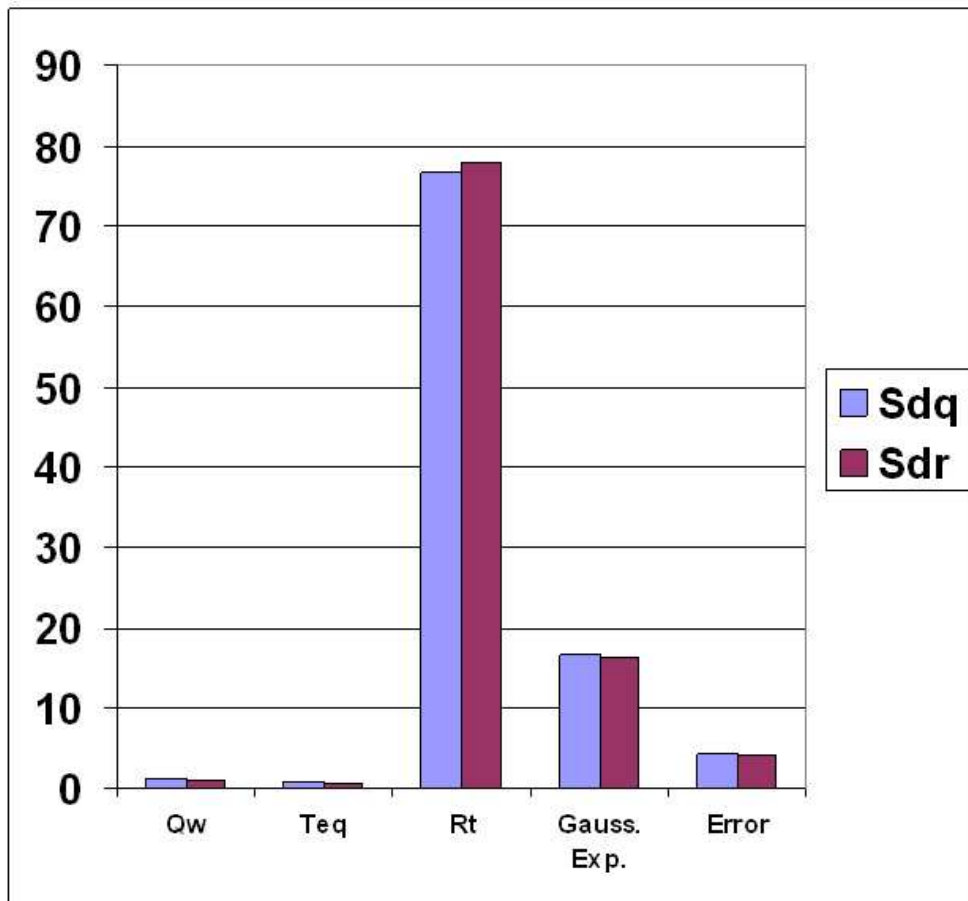


Figure 12. Contribution percents on Sdq and Sdr.
167x155mm (96 x 96 DPI)

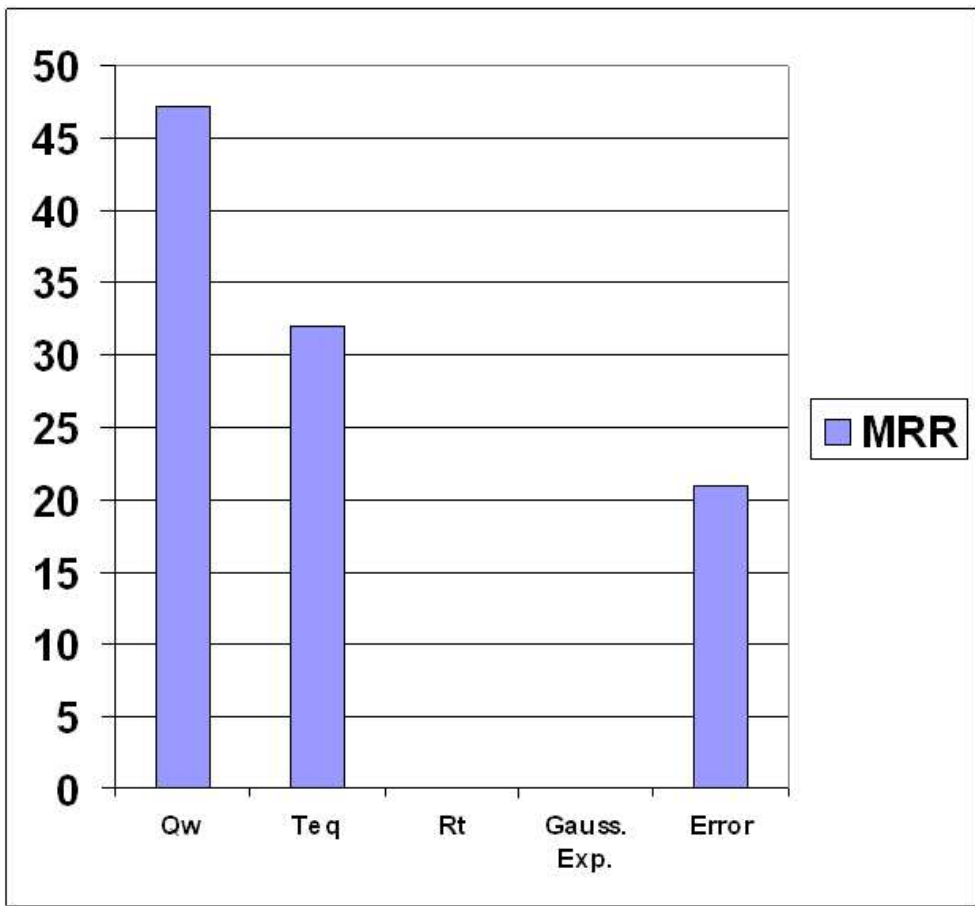


Figure 13. Contribution percents on material removal rate.
167x155mm (96 x 96 DPI)

Only